4540 *Ind. Eng. Chem. Res.* **2004,** *43,* 4540−4550

Advanced Kinetic Concepts and Experimental Methods for Catalytic Three-Phase Processes

Tapio Salmi,* Dmitry Yu. Murzin, Jyri-Pekka Mikkola, Johan Wärnå, Päivi Mäki-Arvela, Esa Toukoniitty, and Sami Toppinen

Laboratory of Industrial Chemistry, Process Chemistry Centre, Åbo Akademi, FIN-20500 Turku/Åbo, Finland

Kinetic studies of catalytic three-phase systems are traditionally performed in autoclaves operating batchwise, and the results are described with rate equations based on the simple Langmuir−Hinshelwood concept. This is not sufficient, as complex organic molecules react on the catalyst surface, and more advanced kinetic models and experimental techniques are needed. Semicompetitive and multicentered adsorption models have been applied to kinetic data, and transient step−response experiments have been carried out for various industrially relevant three-phase systems. The theoretical basis of the advanced kinetic concept is described and successfully applied to several industrially relevant processes, such as hydrogenation of aromatic components and aldehydes on commercial catalysts and enantioselective hydrogenation on modified catalyst surfaces.

Introduction

In the kinetic development process, experimental measurements of reaction rates play a central role. From experimental kinetic data of reaction rates one can, through mathematical modeling, arrive at rate expressions that describe the reaction rate as a function of process parameters, such as temperature, pressure, and concentrations of participating species. The rate equations obtained from kinetic measurements serve both science and engineering. Rate equations describe the underlying molecular-level mechanisms of the reaction; this could be called pure science. In addition, rate equations are of crucial importance for the practical design of chemical reactors operating at the industrial scale. Rate equations are combined with models for mass and heat transfer and models for the flow patterns of the chemical reactor. The result is a complete description of the performance of the reactor. In the present paper, we discuss new trends in kinetics, both rate equations and experimental methods for catalytic three-phase systems, particularly catalytic hydrogenation. For a catalytic three-phase system, the coexistence of kinetic and mass-transfer effects is a profound phenomenon, as illustrated by Figure 1.

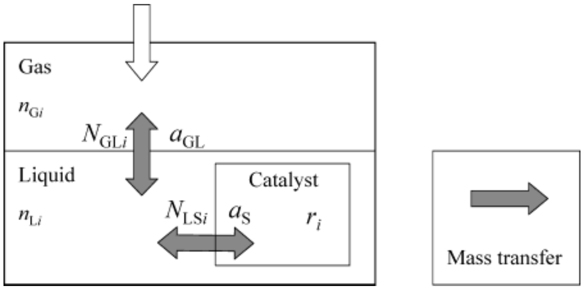

Figure 1. Kinetic and mass-transfer effects in catalytic three-phase systems.

Catalytic liquid-phase hydrogenation is applied in several branches of chemical industry: for example, hydrogenation is used in the production of bulk and fine chemicals. In the field of oil refining, hydrogenation is applied in the manufacturing of aromatic-free solvents and fuels. The production of fine chemicals, e.g., pharmaceuticals and fragrances, is a growing sector that requires the use of catalytic hydrogenation. Furthermore, many well-known alimentary products in our everyday life, such as margarine and alternative sweeteners, are produced via liquid-phase hydrogenation. From the chemical viewpoint, this usually implies the hydrogenation of the aromatic ring, carbonyl group, and/or double bond. Typical catalysts used in liquid-phase hydrogenation belong to the group VIIIA metals, including Ni, Pt, Pd Rh, and Ru, supported on various materials, such as aluminum oxide, silica, active carbon, and different kinds of zeolite materials.

Kinetic Experiments for Three-Phase Systems

Reactors for Batch and Continuous Experiments. A typical kinetic experiment in three-phase hydrogenation is carried out in a slurry reactor (autoclave) operating batchwise. A schematic of a standard experimental device is depicted in Figure 2. Finely dispersed catalyst is poured into the reactor and pretreated under dry conditions with hydrogen, after which the pretreated and hydrogen-saturated solvent is pushed into the reactor vessel. The temperature is adjusted and the substrate, i.e., the reactant, is introduced into the reactor together with a small amount of solvent. The pressure is adjusted to the desired value, and the kinetic experiment can start. In studies with concentrated solutions, the entire amount of the reactant−solvent mixture is preheated separately and fed into the reactor. This is the ideal procedure in kinetic experiments for three-phase hydrogenation. In practice, some compromises are often made; for example, rather than being preheated, the solvent might be poured directly over the catalyst, which introduces an initiation period into the experiment, as the temperature gradually increases to the desired value.

In kinetic experiments carried out in three-phase systems, it is crucial to remove all mass-transfer

---

* To whom correspondence should be addressed. Fax: +358-2-2154479. E-mail: Tapio.Salmi@abo.fi.

10.1021/ie0307481 CCC: $27.50

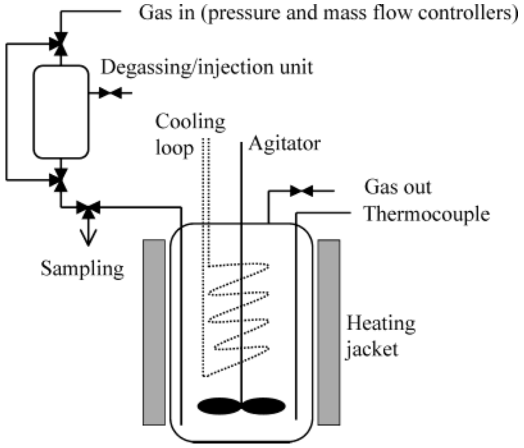

Figure 2. Batch reactor used for kinetic studies of three-phase systems.

resistances, which principally can appear at the gas–liquid interface, at the liquid–solid catalyst interface, and inside the catalyst pores (Figure 1). A classical way to suppress the mass-transfer resistances is to use an efficient stirrer, e.g., a turbine impeller with some modifications (Figure 2), and a sufficiently high agitation velocity. Furthermore, small catalyst particles (on the micrometer scale, typically less than 50 μm) are used to suppress the internal mass-transfer resistance inside the catalyst particles. Typically a series of experiments is carried out with various amounts of catalysts, and also sometimes with different catalyst particle sizes, to ensure the absence of mass-transfer limitations. The details of the criteria developed for mass-transfer limitations are discussed elsewhere (e.g., by Smith[1]).

Autoclaves operating batchwise are the workhorses of kinetic experiments in three-phase systems. Alone, however, they cannot reveal all of the essential features of the catalytic process. Catalyst deactivation is often severe, as complex organic molecules interact with the solid surface. The deactivation is not always directly visible from a kinetic curve obtained from a batch reactor; rather, repeated experiments with recycled catalyst are needed, which significantly retards the kinetic work. Kinetic data on catalytic hydrogenation are often obscured by catalyst deactivation. This can lead to an incorrect interpretation of the kinetic data, particularly if the batchwise experiments in slurry reactors are not supported by experiments in continuous devices. A particularly tricky case is slow deactivation, which is not revealed by simple repetition of the experiment.

Furthermore, a quasi-steady state becomes established on the catalyst surface during long experimental runs in a slurry reactor, which means that a great deal of kinetic information about the reaction mechanism remains beyond the horizon of the experimental observations. For catalytic gas-phase systems, continuous reactors and transient (nonstationary) experiments are well-established and commonly used experimental techniques[2,3] to reveal mechanistic phenomena. Even nonstationary operation of catalytic two-phase reactors is applied.[4,5]

Transient studies of three-phase systems are much more scarce, but still possible. Equipment for transient studies for three-phase systems is depicted in Figure 3. The core of the experimental device is a reactor tube, which is packed with catalyst particles, monoliths, or layers of fibrous catalysts (Figure 3). The liquid and gas flow continuously through the catalyst bed. For slow reactions, the liquid phase can be recirculated. By changing the amount of catalyst and the flow rates, it is possible to investigate the role of external mass-transfer limitations. The length of the bed and the catalyst particle size can be varied to study the pressure drop and internal mass-transfer resistance. The flow pattern can be determined by experiments with inert tracers. It might be the case that all of the mass-transfer resistances are not removed, but the continuous device still provides valuable information about catalyst deactivation and reaction mechanisms. Step changes of the inlet concentrations can easily be established, and their effects on the catalyst performance can be measured.

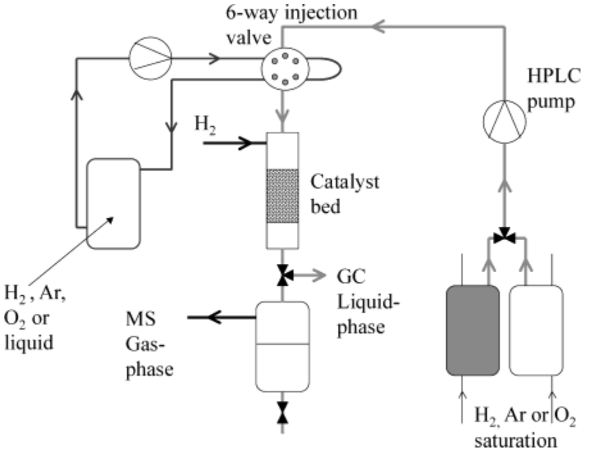

Figure 3. Continuous reactor system used for kinetic studies of three-phase systems.

Experimental Information from Batch and Continuous Reactors. Now, we consider the case of a typical kinetic experiment that has been carried out for liquid-phase hydrogenation in a batch reactor, where several reactions and several components appear simultaneously. Kinetic curve that describing the catalytic hydrogenation of a dione, namely, 1-phenyl-1,2-propanedione, on a modified Pt catalyst are presented in Figure 4a. The decrease of the reactant concentration and the product distribution are observed. Finally, the formation of the ultimate reaction products becomes visible. Kinetic curves of this type measured experimentally are currently very smooth and precise, as automatic and semiautomatic analytical methods have been developed. The experimental results of Figure 4a were obtained from a laboratory-scale slurry reactor with GC analysis and an autosampler. The kinetic curves exhibit some characteristic features: As experiments are carried out at various hydrogen pressures, a first-order dependency on hydrogen pressure, e.g., the concentration of dissolved hydrogen in the liquid phase, typically appears. Furthermore, the reaction order with respect to the organic reactant follows the characteristic pattern that, in the beginning, the reaction order is close to zero, but it gradually increases toward the value of 1.

Results of a kinetic experiment for the same model system but in a continuous reactor (Figure 3) are presented in Figure 4b. Various step changes can be introduced: through the start-up and/or shut-down of the reactor, as well as through pretreatment with a catalyst modifier. As revealed by the figure, new effects become visible in continuous operation: the catalyst is deactivated, and the product distribution is changed

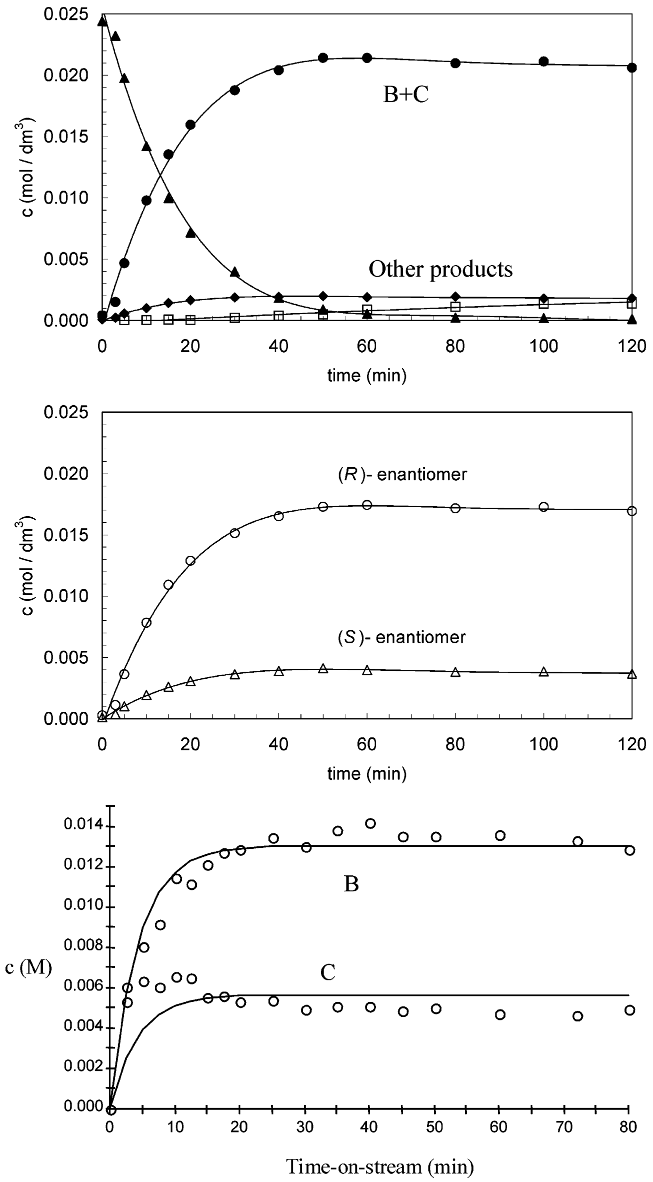

Figure 4. Results from a typical kinetic experiment in (a) batch and (b) continuous reactors for the hydrogenation of 1-phenyl-1,2-propanedione on a modified Pt catalyst. (For the reaction scheme, see Figure 10.)

during the transient period. This information can be used for both qualitative and quantitative treatments, i.e., the estimation of kinetic parameters.

Three-Phase Reactor Models for Kinetic Studies

The model for the test reactor is essential for the planning and interpretation of the experiments, as well as for the estimation of kinetic and mass-transfer parameters from the experimental data. In the following section, we show how the reactor model can be expressed in a general way that is valid for batch and continuous systems. The model is based on the following concepts:[6] the system is dynamic (transient), the mass-transfer resistance is included in three locations (at the gas−liquid and liquid−solid interfaces, as well as inside the catalyst particles), and the flow is described by the plug-flow model with axial dispersion. The catalyst particle is assumed to be completely wetted. The reactor is isothermal, or an experimentally recorded temperature profile is available; thus the energy balance is discarded.

According to Figure 1, the mass balance for component i in the liquid phase can be written as

$$n'_{\mathrm{L}i,\mathrm{in}} + \left(-D_{\mathrm{L}} \frac{\partial c_{\mathrm{L}i}}{\partial l} A\right)_{\mathrm{in}} + N_{\mathrm{L}i}A_{\mathrm{GL}} + \eta_{\mathrm{e}i} r_i m_{\mathrm{cat}} = n'_{\mathrm{L}i,\mathrm{out}} + \left(-D_{\mathrm{L}} \frac{\partial c_{\mathrm{L}i}}{\partial l} A\right)_{\mathrm{out}} + \frac{\partial n_{\mathrm{L}i}}{\partial t} \quad (1)$$

where the symbols are defined in the Notation section. It should be noticed that the overall effectiveness factor in eq 1 accounts for the liquid−solid mass transfer as well as the internal mass transfer (Figure 1). Explicit expressions for the effectiveness factor for simple kinetics are listed in numerous textbooks (e.g., Smith[1]). For complex nonlinear kinetics, a numerical solution of the mass balance of the catalyst pellet is inevitable.[6−9] For the diffusion flux, several approaches exist, from the complete set of Stefan−Maxwell equations to the simple law of Fick.[10,11]

After some rearrangement, the model equation for the liquid phase becomes

$$\frac{\partial c_{\mathrm{L}i}}{\partial t} = (Pe_{\mathrm{L}}\epsilon_{\mathrm{L}}\tau_{\mathrm{L}})^{-1} \frac{\partial {c_{\mathrm{L}i}}^{2}}{\partial z^{2}} - (\epsilon_{\mathrm{L}}\tau_{\mathrm{L}})^{-1} \frac{\partial c_{\mathrm{L}i}}{\partial z} + N_{\mathrm{L}i}a_{\mathrm{v}}/\epsilon_{\mathrm{L}} + \eta_{\mathrm{e}i} r_i \rho_{\mathrm{B}} \quad (2)$$

For the gas phase, an analogous approach is applied, but no reactions are assumed to take place in the gas phase; thus, the mass balance equation becomes

$$\frac{\partial c_{\mathrm{G}i}}{\partial t} = (Pe_{\mathrm{G}}\epsilon_{\mathrm{G}}\tau_{\mathrm{G}})^{-1} \frac{\partial {c_{\mathrm{G}i}}^{2}}{\partial z^{2}} - (\epsilon_{\mathrm{G}}\tau_{\mathrm{G}})^{-1} \frac{\partial c_{\mathrm{G}i}}{\partial z} - N_{\mathrm{L}i}a_{\mathrm{v}}/\epsilon_{\mathrm{G}} \quad (3)$$

Some special cases of eqs 2 and 3 are of interest; for example, for batch reactors operating in the kinetic regime, in the absence of mass-transfer limitations, just the liquid-phase mass balance (eq 2) is needed, and it is compressed to the expression $\mathrm{d}c_i/\mathrm{d}t = \rho_{\mathrm{B}} r_i$.

Kinetic Modeling

The essential part of kinetic modeling is derivation of rate expressions for heterogeneously catalyzed processes. The procedure starts from a presumed or confirmed set of elementary steps, after which some simplifications, such as the concept of rate-determining step, are introduced.[12−14] The result is an explicit rate equation, often referred to as the Langmuir−Hinshelwood−Hougen−Watson (LHHW) expression. Most rate equations presented in chemical engineering literature are still based on the Langmuirian concept of an ideal surface, in which all of the surface sites are uniform and equal from an energy viewpoint. Later, theories taking into account the nonuniformity of the catalyst surface were developed.[15]

LHHW rate equations have proven to be very practical in chemical engineering kinetics, but there are numerous cases for which they are not applicable for physical reasons and, thus, for which they cannot explain kinetic observations. Thus, more advanced kinetic concepts, such as semicompetitive and multicentered adsorption models are needed even in chemical engineering kinetics.

Semicompetitive and Multicentered Adsorption Models. A particular challenge in kinetic studies of three-phase systems is that one cannot screen the entire concentration domain of the gas and the organic components, as can be done for gas-phase systems. That is, the hydrogen solubility significantly limits the concentration of dissolved hydrogen in the liquid phase, which implies, in practice, that one must always operate with a high excess of the organic component in liquid-phase hydrogenation processes.

The researcher is faced with the question of which is the true molecular mechanism on the level of the catalyst surface. Several issues are still unclear or controversial: The mode of hydrogen adsorption is decisive for the formulation of the rate equation. According to classical literature, hydrogen adsorbs dissociatively on many metals, as, for example, is confirmed by fitting the dissociative adsorption model to experimental adsorption isotherms or temperature-programmed desorption data.[13]

It is also known, however, that hydrogen can appear on the catalyst surface in molecular form. Thus, it can be asked whether the dissociative or molecular form of hydrogen is active in hydrogenation. Furthermore, one faces the issue of simultaneous adsorption of hydrogen and organic components on the catalyst surface. Because hydrogen and organic molecules have very different sizes, it might be reasonable to assume that their adsorption on the catalyst surface is mostly noncompetitive in character. However, the assumption of completely noncompetitive adsorption is somewhat artificial from a physical point of view. In this article, we show that it is possible to introduce a semicompetitive adsorption isotherm that describes the fact that, even upon complete adsorption of organic components, some interstitial surface sites remain accessible for the adsorption of the smaller molecule, i.e., hydrogen (semicompetitive adsorption model).

It is reasonable to imagine that that the larger organic molecules need more surface sites than hydrogen. This concept is called the multicentered adsorption of organics on metal sites.[16] Typically, the reaction path on the catalyst surface involves hydrogen adsorption, organics adsorption, surface reaction, and desorption steps. Most rate equations presented in the chemical engineering literature are based on the assumption that the hydrogenation step alone is rate-determining. The experimental evidence for this assumption, however, can be hard to provide. Another possibility is that the hydrogenation step and the organics adsorption together determine the overall reaction rate.

Usually, the adsorption stoichiometry in classical catalysis is assumed to be 1:1, i.e., component A hits a vacant surface site and adsorbs on it. This traditional concept is very fruitful in many fields of catalysis, e.g., in inorganic applications and for small molecules reacting in automotive exhaust catalysts, but organic catalysis is much more complicated. In this case, one must consider various molecular sizes interplaying on the surface, as well as multicentered and semicompetitive adsorption. Furthermore, for multifunctional molecules, the different adsorption modes of the reacting molecule appearing on the catalyst surface should be considered.[17]

Rate Equations for Semicompetitive and Multicentered Adsorption Models. (a) Semicompetitive Adsorption. The concept of semicompetitive adsorption is illustrated in Figure 5. The larger (organic) molecule adsorbs on a cluster of primary sites on the catalyst surface. An arbitrary number of sites can be assumed for the adsorption of the organic molecules, but a preferable way to estimate the size of the adsorption cluster is based on molecular considerations, i.e., the size of the organic molecule and the structure of the catalyst surface. Between the adsorbed molecules remain interstitial sites for the smaller molecule to stick (here, hydrogen), and the maximum coverage of the larger molecule is less than unity because of the greater molecular size. The concept of semicompetitive adsorption has been experimentally verified for the adsorption of aromatics from the gas phase,[18] and the rate equations for a special case, the catalytic hydrogenation of xylose to xylitol, have previously been presented.[19]

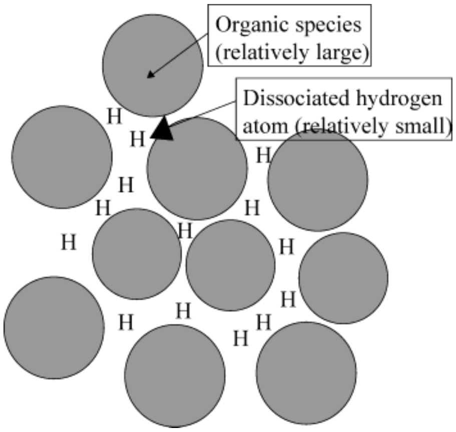

Figure 5. Semicompetitive adsorption.

Here, we derive the rate equation for a general case in which an organic molecule (A) adsorbs on a cluster consisting of *m* primary sites. The small molecule (B, typically hydrogen) adsorbs either in molecular form or dissociatively. The surface reaction between the adsorbed species is rate-limiting. Product molecule adsorption is discarded in the following discussion, because it does not bring theoretically interesting features. The reaction mechanism is written as follows

$$\mathrm{A} + {}' = \mathrm{A}^{*\prime} \qquad \text{(I)}$$

$$\mathrm{B} + i^{*} = i\mathrm{B}^{*} \qquad \text{(II)}$$

$$\mathrm{A}^{*\prime} + j\mathrm{B}^{*} \rightarrow \text{products} + \text{released sites} \qquad \text{(III)}$$

where $*'$ denotes a cluster consisting of *m* primary sites (*).

Consequently, the rate of the surface reaction is given by

$$r = kc_{\mathrm{A}^{*\prime}}c_{\mathrm{B}^{*}}{}^{j} \qquad (4)$$

For the rapid adsorption steps, the quasi-equilibria are expressed by

$$K_{\mathrm{A}} = c_{\mathrm{A}^{*\prime}}/(c_{*\prime}c_{\mathrm{A}}) \qquad (5)$$

and

$$K_{\mathrm{B}} = c_{\mathrm{B}^{*}}{}^{i}/(c_{*}{}^{i}c_{\mathrm{B}}) \qquad (6)$$

The total balance of primary sites is given by

$$c_0 = mc_{\mathrm{A}^{*\prime}} + c_{\mathrm{B}^{*}} + c_{*} \qquad (7)$$

where c_0 is the total concentration of primary sites on the surface.

For the larger molecule (A) the site balance is written as

$$c_{A*'} + c_{*'} = \alpha(c_0 - c_{B*})/m \qquad (8)$$

where α is the adsorption-competition parameter of the larger molecule and $c_{*'}$ is the concentration of vacant clusters accessible for the adsorption of A. The adsorption semi-equilibria in eqs 5 and 6 are inserted into the balance above, and the relationship between the concentrations of vacant clusters ($c_{*'}$) and vacant primary sites (c_*) is obtained as

$$c_{*'} = (\alpha/m)\{[c_0 - (K_B c_B)^{1/i} c_*]/(1 + K_A c_A)\} \qquad (9)$$

This expression is inserted into the balance of primary sites, eq 7. After straightforward algebraic steps, the concentration of vacant primary sites becomes

$$c_*/c_0 = [1 + (1 - \alpha)K_A c_A]/\{(1 + K_A c_A)[1 + (K_B c_B)^{1/i}] - \alpha K_A c_A (K_B c_B)^{1/i}\} \qquad (10)$$

Rate eq 4 can be expressed with the quasi-equilibria in eqs 5 and 6 as

$$r = k K_A K_B^{j/i} c_A c_B^{j/i} c_{*'} c_*^{j} \qquad (11)$$

The expressions for c_* and $c_{*'}$ are inserted into the rate equation, which, after rearrangement, takes the final form

$$r = k(c_0^{j+1}/m) K_A K_B^{j/i} c_A c_B^{j/i} \alpha[1 + (1 - \alpha)K_A c_A]^{j} / [1 + K_A c_A + (K_B c_B)^{1/i} + (1 - \alpha)K_A K_B^{1/i} c_A c_B^{1/i}]^{j+1} \qquad (12)$$

This general rate equation reduces to the standard LHHW rate expression for competitive adsorption on single sites ($\alpha = 1$ and $m = 1$).

(b) Multicentered Adsorption. If multicentered adsorption of a species (A_i) is treated in the classical way, the adsorption step is expressed as

$$A_i + mi* = A_{imi}* \qquad (I')$$

where mi is the number of sites need for the adsorption of A_i. The catalytic steps are thus given, for example, by eq I′ and eqs II and III (listed in the previous section).

Application of the quasi-equilibrium hypothesis to this step implies

$$K_{A_i} = c_{A_i*}^{\ mi}/(c_*^{\ mi} c_{A_i}) \qquad (13)$$

The site balance comprising all of the adsorbing species is written as

$$c_0 = \sum mi\, c_{A_i*'} + c_* \qquad (14)$$

After the adsorption quasi-equilibrium is introduced for each component and c_*/c_0 is denoted as θ, the site balance becomes

$$\sum mi K_{A_i} c_0^{\ mi-1} c_{A_i} \theta^{mi} + \theta = 1 \qquad (15)$$

i.e., a polynomial expression with respect to θ. Analytical solution of eq 15 is easy only for $mi = 1$ and $mi = 2$ (the highest value of mi); for $mi > 3$ and noninteger values of mi, a numerical solution is convenient. Equation 15 is solved iteratively, e.g., by the Newton–Raphson method.

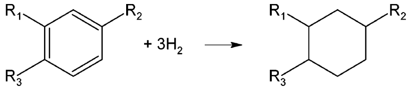

$$R = \frac{k_1 K_A K_{H_2} c_A c_{H_2} \alpha[(1-\alpha)K_A c_A + 1]}{[(1-\alpha)K_A K_{H_2} c_A c_{H_2} + K_A c_A + K_{H_2} c_{H_2} + 1]^2}$$

Figure 6. Reaction scheme for application example a, the hydrogenation of aromatics (toluene and dialkylbenzenes).

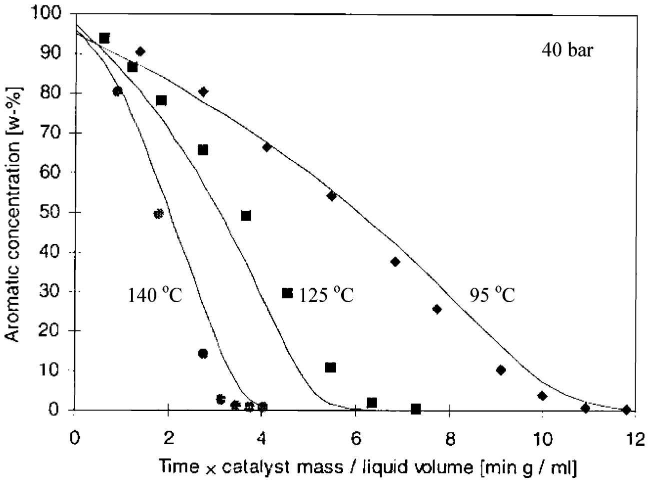

Figure 7. Kinetic modeling for the hydrogenation of aromatics (alkylbenzenes).

Application Examples

Several application examples are considered here, including (a) the hydrogenation of aromatics (alkylbenzenes to alkyl cyclohexanes) and the hydrogenation of the carbonyl group in terms of (b) the hydrogenation of sugars and (c) the enantioselective hydrogenation of aldehydes and ketones. The hydrogenations of aromatics and sugar molecules illustrate the concept of semicompetitive adsorption, whereas enantioselective hydrogenation illustrates multicentered adsorption and the application of transient techniques in kinetic studies. The application examples presented in Figures 6, 8, and 10 are treated in detail in the following sections.

(a) Hydrogenation of Aromatics. Aromatic components are hydrogenated to saturated components to produce aromatic-free solvents and to suppress the contents of aromatics in fuels. A typical catalyst for this process is nickel on alumina. The process can be carried out both in the gas phase and in the liquid phase. Here, we consider the hydrogenation of benzene and some alkylbenzenes to their saturated homologues, as depicted in Figure 6. Kinetic experiments were carried out in a batch reactor over a Ni catalyst.[8] The reaction proceeds on surface nickel in the liquid phase, and typical experimental results are displayed in Figure 7. Principally, the reaction is straightforward: no partially hydrogenated intermediates are visible in the liquid phase, and a relatively constant ratio of the cis and trans isomers of the product, dialkylcyclohexane, is obtained.

The aromatic molecule adsorbs horizontally on the nickel surface. Because the difference in size between the aromatic molecule and hydrogen is considerable, it is reasonable to assume that different numbers of sites

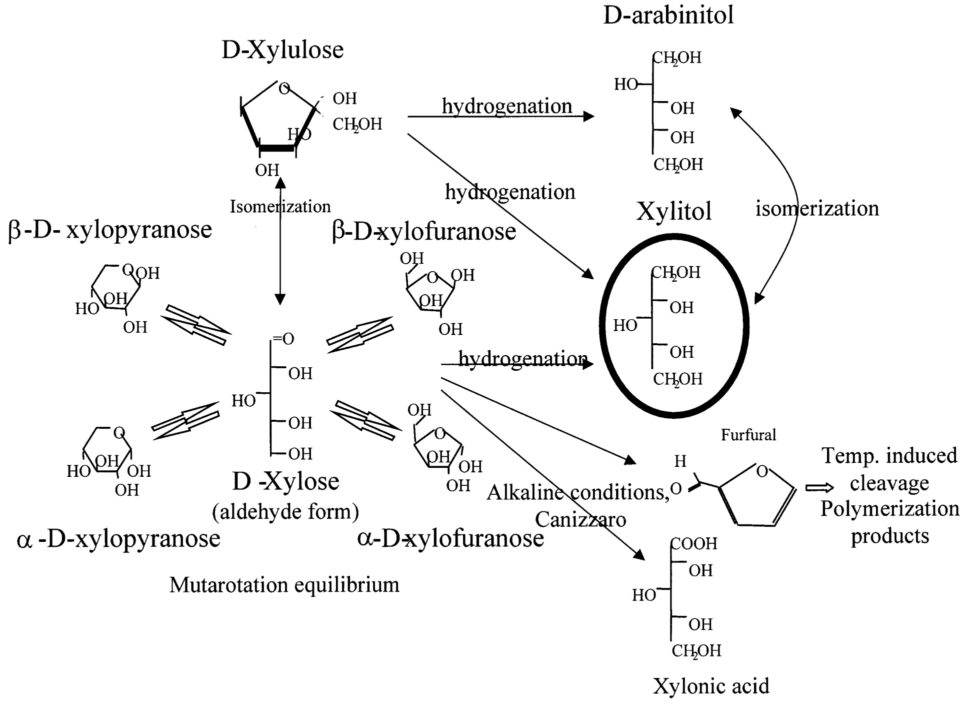

1.) $S + x^{*} \overset{K_S}{\rightleftharpoons} S\,x^{*}$

2.) $H_2 + 2^{*} \overset{K_H}{\rightleftharpoons} 2(H^{*})$

3.) $S \xrightarrow{K_{isom}} X_y$

4.) $X_y + x^{*} \overset{K_{xy}}{\rightleftharpoons} X_y\,x^{*}$

5.) $S\,x^{*} + 2(H^{*}) \xrightarrow{K_{RDS,X1}} \underset{x^{*}}{X} + 2^{*}$

6.) $X_y\,x^{*} + 2(H^{*}) \xrightarrow{K_{RDS,X2}} \underset{x^{*}}{X} + 2^{*}$

7.) $X\,x^{*} \overset{K_X}{\rightleftharpoons} X + x^{*}$

8.) $X_y\,x^{*} + 2(H^{*}) \xrightarrow{K_{RDS,A}} \underset{x^{*}}{A} + 2^{*}$

9.) $A\,x^{*} \overset{K_b}{\rightleftharpoons} A + x^{*}$

10.) $S\,x^{*} \xrightarrow{K_{RDS,F}} F\,x^{*} + 3\,H_2O$

11.) $F\,x^{*} \overset{K_F}{\rightleftharpoons} F + x^{*}$

$$R_1 = \frac{k_d k_{RDS,X1} K_S K_H \alpha \left[1 + (1-\alpha)\Sigma\right]^2 c_H c_S}{\left[(1 + K_H c_H)^{1/j} + \Sigma + (1-\alpha)(K_H c_H)^{1/2}\Sigma\right]^{j+1}}$$

$$\Sigma = (K_S + K_{XY} k_{isom}) c_S + K_A c_A + K_X c_X + K_F c_F$$

α =Fraction of sites covered with organic;
α=1 is the competitive model

S = D-xylose
X_y = D-xylulose
X = xylitol
A = D-arabinitol
H = hydrogen
* = active site
x = number of ads. sites required

Figure 8. Reaction scheme and kinetic model for application example b, the hydrogenation of aldehydes (xylose).

are needed for aromatics adsorption and for hydrogen adsorption. Separate adsorption studies[18] have shown that aromatic molecules do not reach full coverage on the nickel surface. Thus, it is physically reasonable to assume that the adsorption of aromatics and hydrogen is semicompetitive in nature.

Because the cis-to-trans ratio in the product was virtually constant in all of the experiments, the kinetic treatment was simplified by introducing this ratio into the rate equation describing the overall hydrogenation rate, for which the expression obtained for semicompetitive adsorption, eq 12, was used. The interpretation of the kinetic data was complicated by the fact that trilobic catalyst particles (on the millimeter scale) were used, and the data became influenced by internal mass-transfer limitations. The effectiveness factor (η_{ei}, eq 2) was calculated for each component by numerical solution of the transient mass balances of the catalyst particle, i.e., by solution of the partial differential equations describing simultaneous reaction and diffusion in the particle. The textural properties of the catalyst were known, and the diffusion coefficients of the compounds were calculated from the Fuller–Schettler–Giddings equation[20] a priori. Thus, only the kinetic parameters were determined by regression analysis from the experimental data.

Some examples of data fitting are displayed in Figure 7. It was concluded that the model predictions follow the experimental data faithfully.

(b) Hydrogenation of Aldehydes. The example of carbonyl group hydrogenation of aldehydes concerns the hydrogenation of sugars. Xylitol is a sweetening agent, the raw material of which is obtained, for example, from a tree, birch (*Betula*). The hemicellulose appearing in birch, arabinogluguronoxylane, is hydrolyzed under strongly acidic conditions, with the xylose molecule being obtained as a hydrolysis product. To obtain a sweet taste, it is necessary to hydrogenate the carbonyl group of xylose to give the xylitol molecule. The reaction scheme is displayed in Figure 8. In the hydrogenation of xylose, several chemical phenomena that are characteristic for sugar molecules occur. Hydrogenation, isomerization, and mutarotation result in complex solution behavior. In this case, we applied the semicompetitive adsorption model for the adsorption of xylose and hydrogen. Furthermore, the system exhibits profound catalyst deactivation.[19]

A typical industrial catalyst is Raney nickel, but many other catalysts, such as supported nickel on alumina, Rh, and Ru, can also work as hydrogenation catalysts. The characteristic features are the adsorption of hydrogen and the organic molecule. In addition, the raw

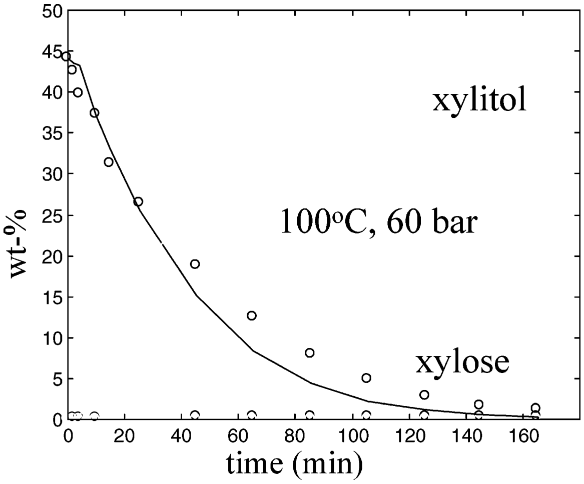

Figure 9. Kinetic modeling for the hydrogenation of sugars (xylose).

material, xylose, undergoes a side reaction, namely, isomerization to form xylulose as a side product. Another byproduct is arabinitol, which can be obtained by the hydrogenation of xylulose or xylose. Under extreme conditions, at high temperatures, even furfural can be observed as a side product. The above discussion shows that optimization of the reaction conditions is of crucial importance in the industrial production of xylitol. In this case, we applied the semicompetitive adsorption model for the adsorption of xylose and hydrogen. The final rate expression according to the semicompetitive model is included in Figure 8.

The characteristic feature in the modeling is the competitiveness factor (α), which is equal to 1 for the classical competitive adsorption model but is less than 1 for the semicompetitive adsorption model. As the surface is fully covered by the organic molecule, $\alpha < 1$, and some interstitial adsorption sites are free for hydrogen to enter. The rate expression presented in the previous section is based on the assumption that the adsorption and desorption steps are rapid compared to the surface reaction step. This model was successfully fitted to the experimental data; some examples of the model fits are displayed in Figure 9. It can be concluded that the semicompetitive adsorption model describes well the disappearance of the reactant molecule (xylose), as well as the product distribution.

In this kind of modeling, it is not sufficient that the rate equations describe well the experimental data for the main components; they must be able to predict the behavior of the byproducts as well. The concentrations of these byproducts are highly important for the industrial production of alimentary products, for which a high degree of purity is required. The model was used to improve the operation of existing xylitol manufacturing plants.

(c) Enantioselective Hydrogenation. This example concerns multicentered adsorption and multifunctional molecules appearing in enantioselective hydrogenation, which is used to produce optically pure isomers needed, for example, in the pharmaceutical industry: typically, only one of the optical isomers (enantiomers) has a therapeutic effect, whereas the other one is useless or even harmful. A conventional heterogeneous catalyst yields a 50:50 mixture of optical isomers in hydrogenation, and a purification step follows the reaction step. It is possible, however, to steer the hydrogenation on heterogeneous catalysts toward one enantiomer by introducing a modifier component, typically an alkaloid on the catalyst surface.[21] The modifier adsorbs on the surface, affecting the reactant absorption in such a way that an excess of one of the enantiomers is obtained in hydrogenation. The enantioselective hydrogenations of two model molecules, 1-phenyl-1,2-propanedione and ethyl puruvate, are considered in batch and continuous systems.

The enantioselective hydrogenation of 1-phenyl-1,2-propanedione, the intermediate for the synthesis of the well-known drug ephedrine, follows the reaction scheme depicted in Figure 10. The main product over a Pt-catalyst modified by cinchoninide is the R isomer of 1-phenyl-1-hydroxy-2-propanone, i.e., molecule **B** in the reaction scheme. The product formed in parallel is the S isomer of the same molecule, molecule **C** in the reaction scheme. Because two carbonyl groups are present in the reactant molecule, regioselective aspects play a role as well. The carbonyl group in position 1 can be hydrogenated first, and then carbonyl group 2 is hydrogenated further, giving products **D** and **E** as side products. For extremely long reaction times, the completely hydrogenated diols are obtained (Figure 11). A typical kinetic curve displaying the events according to the reaction scheme was presented in Figure 4.

A characteristic feature for this system is that the reactant molecule has two adsorption modes, one perpendicular and one parallel, as illustrated in Figure 10. The parallel mode implies interaction of the phenyl ring directly with the surface. This form requires more space and favors the hydrogenation of the carbonyl group in position 1. As more of the reactant is added to the system, the adsorption equilibrium is shifted from the parallel mode toward the tilted mode, and the amount of products **D** and **E** is increased.

The concept of multicentered adsorption implies that the parallel adsorption form of the reactant requires more sites than the tilted one and that, when more of the reactant molecule if present, the adsorption is shifted toward the form that requires less space. This hypothesis has been experimentally confirmed, and it also reflects the product distribution, namely, the regioselectivity of the products during the reaction. The influence of the reactant concentration on the adsorption mode is illustrated in Figure 11, which shows the regioselectivity and enantiomeric excess as functions of the reactant conversion. In addition, the multicentered adsorption concept is applied on the large modifier (cinchoninide) molecule.

Attempts to describe the behavior of the system by simple LHHW models failed mainly because those models were not able to describe the change of regio- and enantioselectivity as a function of the modifier concentration. The advanced kinetic model for carbonyl group hydrogenation for 1-phenyl-1,2-propanedione was based on the following concepts: multicentered adsorption (see eqs 13−15), coadsorption of the organic molecules, and use of a catalyst modifier. One form of the catalyst modifier was not acting in the reaction, but remained as a passive spectator on the catalyst surface. The adsorption of hydrogen was assumed to be essentially noncompetitive: in the experiments, there was no clear dependence of the hydrogenation rate on the hydrogen partial pressure. In this case, the concept of multicentered adsorption is utilized, and although it is

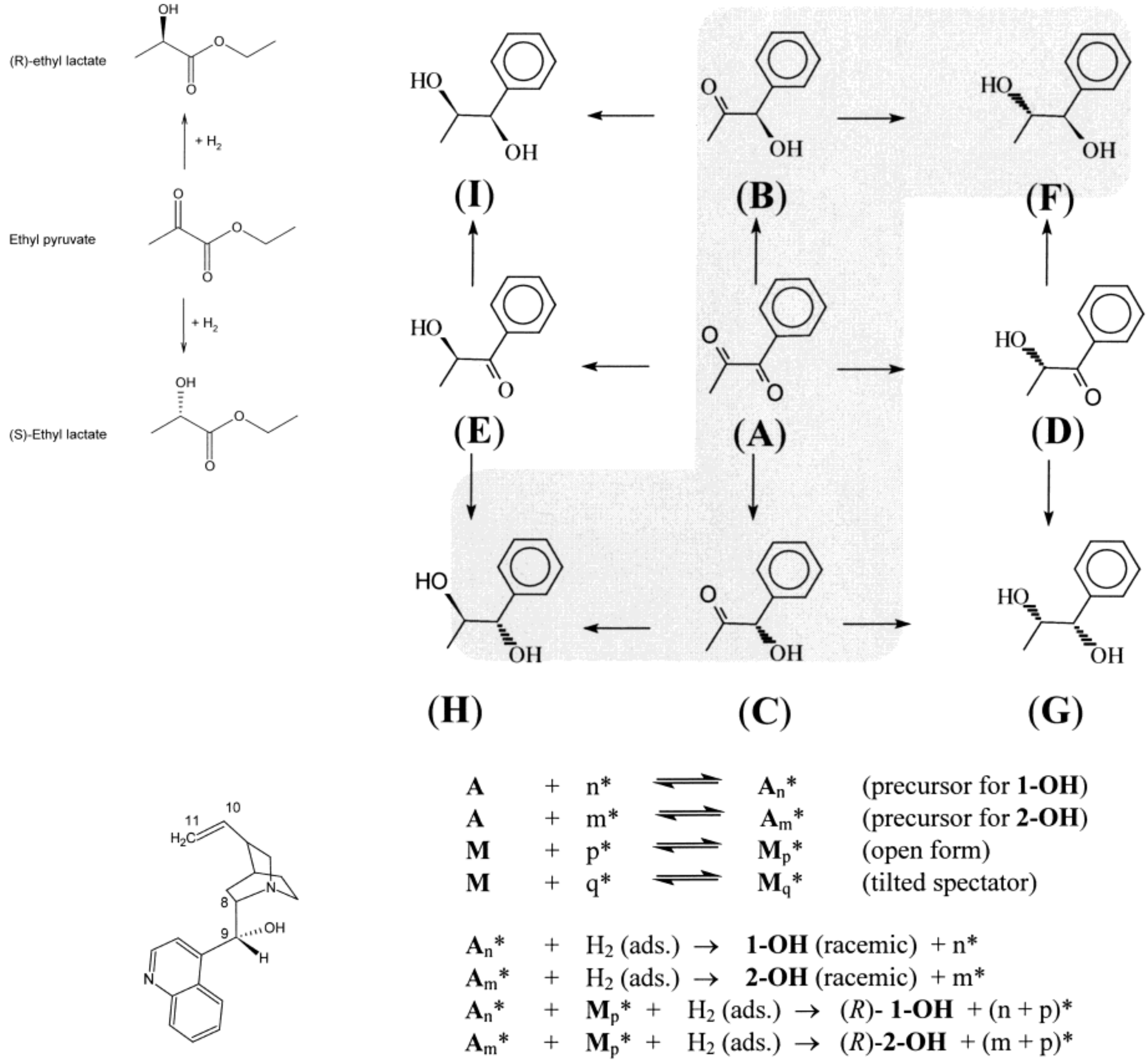

$A + n^* \rightleftharpoons A_n^*$ (precursor for **1-OH**)
$A + m^* \rightleftharpoons A_m^*$ (precursor for **2-OH**)
$M + p^* \rightleftharpoons M_p^*$ (open form)
$M + q^* \rightleftharpoons M_q^*$ (tilted spectator)

$A_n^* + H_2$ (ads.) → **1-OH** (racemic) $+ n^*$
$A_m^* + H_2$ (ads.) → **2-OH** (racemic) $+ m^*$
$A_n^* + M_p^* + H_2$ (ads.) → (*R*)- **1-OH** $+ (n + p)^*$
$A_m^* + M_p^* + H_2$ (ads.) → (*R*)-**2-OH** $+ (m + p)^*$

Figure 10. Reaction scheme and kinetic model for application example c, enantioselective hydrogenation. In the reaction scheme for 1-phenyl-1,2-propanedione hydrogenation, **A** = 1-phenyl-1,2-propanedione, **B** = (*R*)-1-hydroxy-1-phenylpropanone, **C** = (*S*)-1-hydroxy-1-phenylpropanone, **D** = (*S*)-2-hydroxy-1-phenylpropanone, **E** = (*R*)-2-hydroxy-1-phenylpropanone, **F** = (1*R*,2*S*)-1-phenyl-1,2-propanediol, **G** = (1*S*,2*S*)-1-phenyl-1,2-propanediol, **H** = (1*S*,2*R*)-1-phenyl-1,2-propanediol, and **I** = (1*R*,2*R*)-1-phenyl-1,2-propanediol.

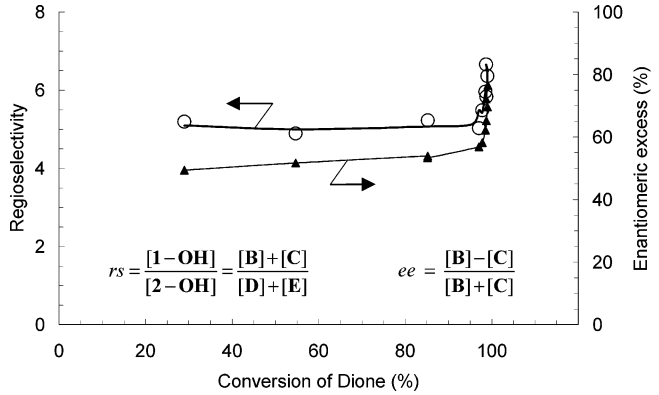

$$rs = \frac{[1-OH]}{[2-OH]} = \frac{[B]+[C]}{[D]+[E]} \qquad ee = \frac{[B]-[C]}{[B]+[C]}$$

Figure 11. Enantiomeric excess (ee) and regioselectivity (rs) for the enantioselective hydrogenation of 1-phenyl-1,2-propanedione.

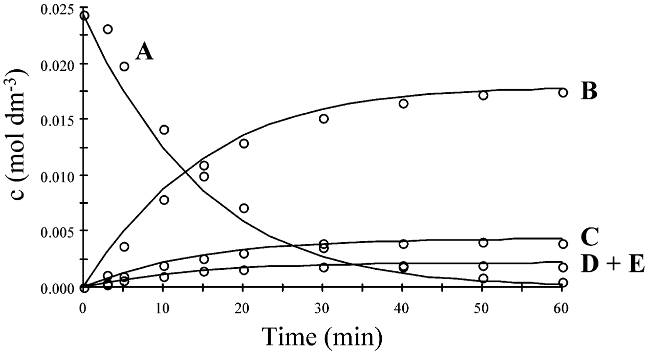

Figure 12. Kinetic modeling based on batch reactor data for the enantioselective hydrogenation of 1-phenyl-1,2-propanedione.

impossible to obtain explicit rate expressions, the fractional coverages are solved numerically from the site balance, as discussed previously. Then, the rate of each step can be calculated, and rate constants can be adjusted by parameter estimation. The complete kinetic model is presented in Figure 10. In Figure 12, the results from parameter estimation are displayed as a function of the reaction time. The results clearly demonstrate that the multicentered adsorption concept works well for this complex hydrogenation system.

For complex organic processes, such as enantioselective hydrogenation, batch experiments alone cannot confirm the reaction mechanism, as a pseudo-steady state is established on the catalyst surface. Therefore, transient experiments were carried out in a continuous reactor system (Figure 3), to reveal the details of the hydrogenation of 1-phenyl-1,2-propanedione and an-

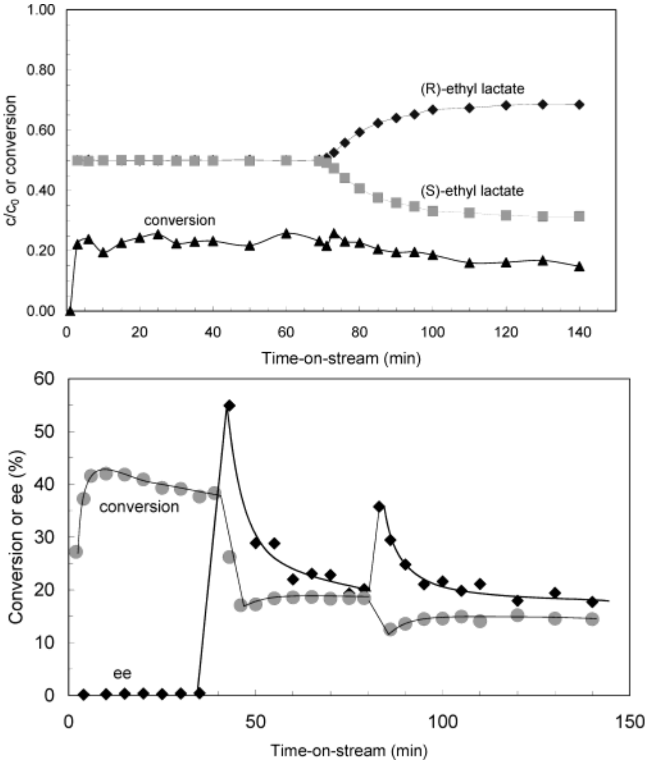

Figure 13. Transient experiments [(a) step responses and (b) pulse experiments] for the enantioselective hydrogenation of ethyl puruvate.

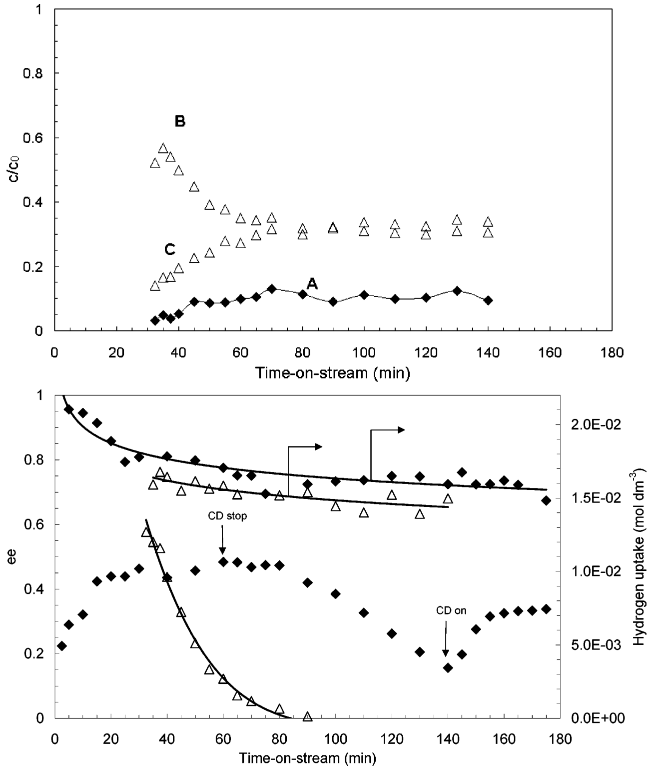

Figure 14. Transient experiments [(a) step responses and (b) pulse experiments] for the enantioselective hydrogenation of 1-phenyl-1,2-propanedione.

other molecule, ethyl puruvate. Ethyl puruvate is a very common model molecule for enantioselective hydrogenation (Figure 10).

Typical qualitative aspects to be revealed by transient experiments in enantioselective hydrogenation include the catalyst stability and the effect of the modifier on the enantioselectivity. The results of transient experiments carried out for ethyl puruvate and 1-phenyl-1,2-propanedione are displayed in Figures 13 and 14, respectively. Hydrogenation of ethyl puruvate over a cinchona-modified Pt−silica fiber catalyst gives the R and S isomers of ethyl lactate as reaction products (Figure 10). The reaction was initiated without the modifier, and a racemic mixture of the products was observed (Figure 13a). Furthermore, the catalyst preserved its stability rather well, as can be seen from the conversion depicted in Figure 13. In the next stage, the flow of the catalyst modifier (cinchoninide) was switched on: the feature of enantioselectivity emerged, and catalyst deactivation became observable (Figure 13a). The effect of the modifier was investigated further by pulse experiments: the reaction was allowed to attain the steady state in the absence of the modifier, after which a small pulse of the modifier was injected (Figure 13b). The enantiomeric excess became immediately visible, but declined as the modifier pulse was flushed from the system.

Two kinds of transient experiments were carried out with 1-phenyl-1,2-propanedione. In the first experiment, the catalyst was pretreated with modifier, after which the reactant feed was switched on and the modifier feed was stopped. In the second experiment, no pretreatment was applied, but the reactant and modifier feeds were commenced simultaneously. The results depicted in Figure 14 clearly reveal the role of the modifier and the progress of catalyst deactivation. The catalyst is slowly but continuously deactivated during the experiment—an effect that easily can remain unobserved in batch experiments. As the modifier was preadsorbed, the enantioselectivity was high from the very beginning, but it declined rapidly because no additional modifier was fed into the system (Figure 14). In the second experiment, the enantioselectivity developed gradually, as the modifier adsorbed on the surface. Catalyst deactivation, however, started immediately, indicating that it is caused by the reactant, not by the modifier.

The discussion above indicates how valuable qualitative information can be obtained form transient experiments performed in three-phase systems. However, the ultimate goal is to describe the observations quantitatively. Thus, the kinetic model for the enantioselective hydrogenation of 1-phenyl-1,2-propanedione (Figure 10) was used to estimate rate parameters for the system. The axial dispersion model, eq 2, was applied to the liquid phase, but the gas-phase balance, eq 3, was discarded, given that the influence of hydrogen on the kinetics was minor under the actual experimental conditions. Two approaches were compared: the pseudo-steady state model with adsorption quasi-equilibria was used in preliminary data fitting, followed by the complete transient model with dynamic adsorption steps. It turned out that the pseudo-steady-state model was able to describe the steady state, but not the transient regime of the experiments. The dynamic model, on the other hand, gave a reasonable description of the transient behavior of the system, as illustrated in Figure 15. The main obstacle in the use of completely dynamic models in practice is the high number of adjustable parameters in regression; therefore, a fruitful approach combines (pseudo-) steady-state experiments with transient kinetic and adsorption studies. In this way, statistically and thermodynamically relevant parameter values can be obtained.

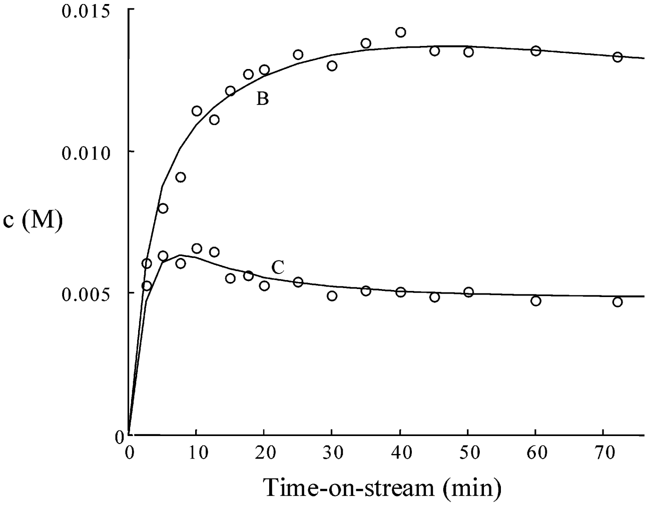

Figure 15. Kinetic modeling based on transient experiments for the enantioselective hydrogenation of 1-phenyl-1,2-propanedione.

Conclusions

Conventional kinetic models and experimental techniques are not sufficient to describe the behavior of complex organic molecules reacting in three-phase catalytic processes. Batch experiments can successfully be supported by transient step−response and pulse experiments to reveal catalyst deactivation along with mechanistic details at the catalyst surface. Advanced concepts in catalytic kinetics, such as semicompetitive and multicentered adsorption models, were described herein, and a new, generally applicable rate equation including semicompetitive adsorption was presented. Transient techniques are extremely informative for catalytic three-phase systems: they reveal important qualitative information about reaction mechanisms and catalyst deactivation, but they can also be used for quantitative modeling of experimental data, as demonstrated by the application examples. Quantitative modeling is the key for successful process design.

Acknowledgment

This work is part of the activities at the Åbo Akademi Process Chemistry Centre within the Finnish Centre of Excellence Programme (2000−2005) of the Academy of Finland.

Notation

A = reactor cross section
A_{GL} = gas−liquid mass-transfer area
a_v = gas−liquid interfacial area-to-reactor volume ratio
c = concentration
c_0 = concentration of surface sites
D = axial dispersion coefficient
K = adsorption equilibrium parameter
k = rate constant
L = reactor length
l = reactor length coordinate
m, mi = number of sites needed for adsorption
m_{cat} = mass of catalyst
N = flux
n = amount of substance
n' = flow of amount of substance (molar flow)
Pe = Peclet number, $Pe = wL/D$
r = rate
t = time
V = volume
w = fluid velocity
z = dimensionless length coordinate, $z = l/L$

Greek Letters

α = competitiveness factor of a large molecule
ϵ = hold-up
η = effectiveness factor
θ = fractional coverage
ρ_B = catalyst bulk density, $\rho_B = m_{cat}/V_L$
τ = space time

Subscripts and Superscripts

e = effectiveness
G = gas
i = component index
j = number of sites in adsorption
L = liquid
*, *′ = vacant site

Literature Cited

(1) Smith, J. M. *Chemical Engineering Kinetics*, 3rd ed.; McGraw Hill: New York, 1990.

(2) Kobayashi, H; Kobayashi, M. Transient response method in heterogeneous catalysis. *Catal. Rev.-Sci. Eng.* **1974**, *10*, 1139−1176.

(3) Bennett, C. O. Experiments and processes in the transient regime for heterogeneous catalysis. *Adv. Catal.* **2002**, *44*, 330−416.

(4) Matros, Yu. Sh. *Unsteady Processes in Catalytic Reactors*; Elsevier: Amsterdam, 1985.

(5) Eigenberger, G.; Nieken, U. Katalytische Abluftreinigung: verfahrenstechnische Aufgaben und neue Lösungen. *Chem. Ing. Tech.* **1991**, *63*, 781−791.

(6) Salmi, T.; Wärnå, J.; Toppinen, S.; Rönnholm, M.; Mikkola, J.-P. Dynamic modelling of catalytic three-phase reactors for hydrogenation and oxidation processes. *Braz. J. Chem. Eng.* **2000**, *17*, 1023−1035.

(7) Rönnholm, M. R.; Wärnå, J.; Salmi, T. Two- and three-phase oxidation of ferrous sulfate to ferric sulfate−From intrinsic kinetics to diffusion-affected kinetics. *Chem. Eng. Process.* **2002**, *41*, 753−760.

(8) Toppinen, S.; Rantakylä, T.-K.; Salmi, T.; Aittamaa, J. Kinetics of the liquid-phase hydrogenation of benzene and some monosubstituted alkylbenzenes over a Ni catalyst. *Ind. Eng. Chem. Res.* **1996**, *35*, 1824−1833.

(9) Toppinen, S.; Salmi, T.; Rantakylä, T.-K.; Aittamaa, J. Liquid-phase hydrogenation kinetics of aromatic hydrocarbon mixtures. *Ind. Eng. Chem. Res.* **1997**, *36*, 2101−2109.

(10) Taylor, R.; Krishna, R. *Multicomponent Mass Transfer*; Wiley: New York, 1993.

(11) Fott, P.; Schneider, P. Multicomponent mass transport with complex reaction in porous catalyst. In *Recent Advances in the Engineering Analysis of Chemically Reacting Systems*; Doraiswamy, L. K., Ed.; Wiley Eastern: New Dehli, India, 1984.

(12) Berger, R. J.; Stitt, E. H.; Marin, G. B.; Kapteijn, F.; Moulijn, J. A. Chemical reaction kinetics in practice. *CATTECH* **2000**, *4*, 2−32.

(13) Boudart, M.; Djéga-Mariadassou, G. *Kinetics of Heterogeneous Catalytic Reactions*; Princeton University Press: Princeton, NJ, 1984.

(14) Laidler, K. J. *Chemical Kinetics*; Harper & Row: New York, 1987.

(15) Temkin, M. I. The kinetics of some industrial heterogeneous catalytic reactions. *Adv. Catal.* **1979**, *28*, 173−292.

(16) Snagovskii, Yu. S.; Ostrovskii, G. M. *Modeling of Kinetics of Heterogeneous Catalytic Processes*; Chimia: Moscow, USSR, 1976 (in Russian).

(17) Toukoniitty, E.; Sevcikova, B.; Mäki-Arvela, P.; Wärnå, J.; Salmi, T.; Murzin, D. Yu. Kinetics and modeling of 1-phenyl-1,2-propanedione hydrogenation. *J. Catal.* **2003**, *213*, 7−16.

(18) Murzin, D.; Salmi, T.; Smeds, S.; Laatikainen, M.; Mustonen, M.; Paatero, E. Toluene and methylcyclohexane adsorption on nickel catalysts. *React. Kinet. Catal. Lett*. **1997**, *61*, 227−236.

(19) Mikkola, J.-P.; Vainio, H.; Salmi, T.; Sjöholm, R.; Ollonqvist, T.; Väyrynen, J. Deactivation kinetics of Mo-promoted Raney Ni catalyst in the hydrogenation of xylose to xylitol. *Appl. Catal. A* **2000**, *196*, 143−155.

(20) Reid, R. C.; Prausnitz, J. M.; Poling, B. E. *The Properties of Gases and Liquids*; McGraw Hill: New York, 1988.

(21) Blaser, H.-U.; Jalett, H.-P.; Wiehl, J. *J. Mol. Catal.* **1996**, *107*, 85.

Received for review October 6, 2003
Revised manuscript received January 16, 2004
Accepted January 22, 2004

IE0307481